DOI: 10.1002/chem.200600897

Synthesis and Characterisation of Nonclassical Ruthenium Hydride Complexes Containing Chelating Bidentate and Tridentate Phosphine Ligands

Martin H. G. Prechtl,[a, b] Yehoshoa Ben-David,[c] Daniela Giunta,[a, b] Stefan Busch,[b] Yuki Taniguchi,[b] Wolfgang Wisniewski,[b] Helmar Görls,[d] Richard J. Mynott,[b] Nils Theyssen,[b] David Milstein,[c] and Walter Leitner*[a, b]

Abstract: The synthesis and characterisation of nonclassical ruthenium hydride complexes containing bidentate PP and tridentate PCP and PNP pincer-type ligands are described. The mononuclear and dinuclear ruthenium complexes presented have been synthesised in moderate to high yields by the direct hydrogenation route (one-pot synthesis) or in a two-step procedure. In both cases [Ru(cod)-(metallyl)$_2$] served as a readily available precursor. The influences of the coordination geometry and the ligand framework on the structure, binding, and chemical properties of the M–H$_2$ fragments were studied by X-ray crystal structure analysis, spectroscopic methods, and reactivity towards N$_2$, D$_2$, and deuterated solvents.

Keywords: chelates · dihydrogen complexes · hydrides · phosphine ligands · ruthenium

Introduction

The discovery of stable transition-metal complexes with molecular dihydrogen as a side-on bound ligand by Kubas et al. in 1983 was a breakthrough in the historical development of coordination chemistry.[1] Since then, dihydrogen complexes of transition metals have been the subject of considerable interest because they present models for the metal-induced activation of the hydrogen molecule,[2–4] either through oxidative addition or heterolytic cleavage.[2,3,5–8] In general, it is possible to obtain nonclassical metal–hydride complexes by direct reaction with hydrogen, by protonation of hydride complexes, or by reduction reactions.[3b] Stable coordination between the molecular dihydrogen and a metal centre is based on two contributions: the donation from the filled H$_2$ σ orbital to the empty d orbitals on the metal, and the back-bonding of the d electrons to the antibonding σ* orbital of the hydrogen ligand. Thus, several factors, such as the ability of the metal to donate electrons and the nature of the ligand in the trans position, influence the stability and the reactivity of the M–H$_2$ unit.[3,4,9] As recently highlighted by van Leeuwen et al., the structural demands of an ancillary chelating ligand can also play an important role in defining the properties of η^2-H$_2$ ligand.[10] In the present paper, we report on the synthesis and characterisation of new nonclassical ruthenium hydride complexes with constrained ligand geometries, which substantiate the importance of well-defined structural features for the H$_2$-binding mode and reactivity.[11]

The chemistry of ruthenium complexes containing nonclassical hydride ligands was pioneered by Chaudret et al. with the synthesis of the hexahydride complex of formula

[a] Dipl.-Chem. M. H. G. Prechtl, Dr. D. Giunta, Prof. Dr. W. Leitner
Institute of Technical and Macromolecular Chemistry
RWTH Aachen University
Worringer Weg 1, 52074 Aachen (Germany)
Fax: (+49) 241-802-2177
E-mail: leitner@itmc.rwth-aachen.de

[b] Dipl.-Chem. M. H. G. Prechtl, Dr. D. Giunta, Dr. S. Busch, Dr. Y. Taniguchi, W. Wisniewski, Dr. R. J. Mynott, Dr. N. Theyssen, Prof. Dr. W. Leitner
Max-Planck-Institut für Kohlenforschung
Kaiser-Wilhelm-Platz 1
45470 Mülheim/Ruhr (Germany)

[c] Y. Ben-David, Prof. Dr. D. Milstein
Department of Organic Chemistry
Weizmann Institute of Science
76100 Rehovot (Israel)

[d] Dr. H. Görls
Institut für Anorganische und Analytische Chemie
Friedrich-Schiller-Universität Jena
Carl-Zeiss Promenade 10, 07745 Jena (Germany)

Supporting information for this article is available on the WWW under http://www.chemeurj.org/ or from the author.

$[Ru(H_2)_2(H)_2(PCy_3)_2]$ (**1**) (Cy = cyclohexyl, Figure 1).[12] This species was proven to possess a unique structure with two classical hydrides and two molecular dihydrogen ligands in mutually *cis* positions,[12c] as confirmed most recently by neutron diffraction for $[Ru(H_2)_2(H)_2(PCyp_3)_2]$ (Cyp = cyclopentyl).[12d] Meanwhile, several ruthenium complexes containing nonclassical hydride ligands have been synthesised, allowing a better understanding of the stability, reactivity, and binding mode of the η^2-H_2 moiety.[13,14] Complex **1** has found application as a starting material for a variety of ruthenium–dihydrogen complexes.[13–15] Moreover, it has been used as a catalyst precursor for hydrogenation,[13,16] silylation,[17] coupling reactions (Murai reaction),[15,18] and metathesis.[19]

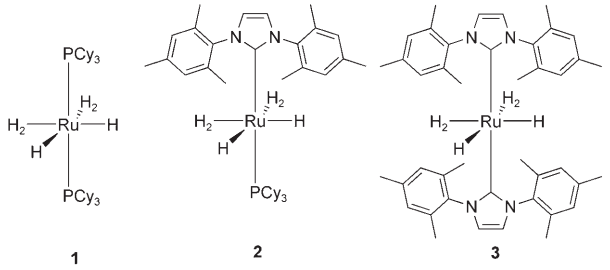

Figure 1. $[Ru(H_2)_2(H)_2(PCy_3)_2]$ (**1**), $[Ru(H_2)_2(H)_2(PCy_3)(IMes)]$ (**2**), $[Ru(H_2)_2(H)_2(IMes)_2]$ (**3**).

Recently, we reported the synthesis of new complexes **2** and **3**, in which one or both PCy_3 ligands of **1** are replaced with strongly basic and sterically encumbered heterocyclic carbene ligands.[20] X-ray crystal structure analysis revealed that the arrangement of the central RuH_6 core is largely retained in these species. However, as a result of the specific ligand environment, the reactivity of the carbene differs from that of **1**, including an interesting potential use in catalytic H/D exchange processes.[20,21] An alternative possibility for expansion of the structural variety of nonclassical ruthenium–hydride complexes is to incorporate the donor sites into chelating frameworks with constrained geometries.[10] In the present work, we have therefore set out to investigate more systematically bi- and tridentate chelating ligand frameworks for the stabilisation of bi- and mononuclear ruthenium dihydrogen complexes (Figure 2).

Preliminary studies from our team[11] and in industrial laboratories[16] indicate that binuclear complexes of the general formula $[Ru_2H_6(P_2)_2]$ can be obtained with chelating ligands P_2 of type $R_2P(CH_2)_nPR_2$. Herein, we describe the synthesis of ruthenium complexes $[H(P_2)Ru(\mu\text{-}H)_3Ru(P_2)(H_2)]$ (**4a**: P_2 = $Cy_2P(CH_2)_3PCy_2$ dcpp; **4b**: P_2 = $Cy_2P(CH_2)_2PCy_2$ dcpe) and the complete spectroscopic and crystallographic characterisation of **4a**. The ligands were chosen to largely retain the electronic nature of the ligands in **1** while enforcing a *cis* geometry with a defined P-M-P angle to allow systematic comparison with similar dinuclear ruthenium complexes previously reported in the literature. To obtain mononuclear structures we have applied PCP and PNP pincer ligands in complexes **5** and **6**, respectively, to force a meridional tridentate coordination mode. Owing to their interesting catalytic behaviour, transition-metal complexes containing tridentate pincer ligands have been studied extensively during the past decade.[22] However, there are limited examples of ruthenium-centred complexes, and no ruthenium dihydrogen complexes with such ligands have been reported so far. In contrast, a number of rhodium, platinum, and osmium complexes containing these pincer ligands are known.[22,23] Recently, a ruthenium dihydrogen complex bearing an aliphatic POP pincer was presented.[23f]

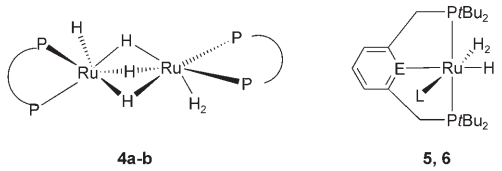

Figure 2. Binuclear complexes **4** and pincer-typed mononuclear complexes **5** and **6**. P∩P = Cy_2P-$(CH_2)_n$-PCy_2; **4a** $[Ru_2H(\mu\text{-}H)_3(H_2)(dcpp)_2]$, n = 3, (dcpp = 1,3-bis(dicyclohexylphosphino)propane); **4b** $[Ru_2H(\mu\text{-}H)_3(H_2)(dcpe)_2]$, n = 2, (dcpe = 1,2-bis(dicyclohexylphosphino)ethane); **5** (E = C; L = H_2): [Ru(dtbpmb)$(H_2)_2$H], (dtbpmb = 1,3-bis(di-*tert*-butylphosphinomethyl)benzol); **6** (E = N; L = H): [Ru(dtbpmp)$H_2(H_2)$], (dtbpmp = 1,3-bis(di-*tert*-butylphosphinomethyl)pyridine).

Results and Discussion

Complexes **4a** and **4b** are readily obtained by hydrogenation of the allyl complexes **7a** and **7b** following a procedure previously developed in our group (Scheme 1).[11,24] Under optimised conditions, **4a** and **4b** have been isolated in fair to excellent yields as orange microcrystalline solids directly from the reaction mixture upon cooling and filtration. Complex **4a** shows high solubility in aromatic solvents and is remarkably stable in the solid state, even in the presence of air or under vacuum. Although the compounds are too thermally labile to detect the molecular ions directly, the fragmentation observed in mass spectroscopic analysis confirms a dinuclear structure for complex **4a**.

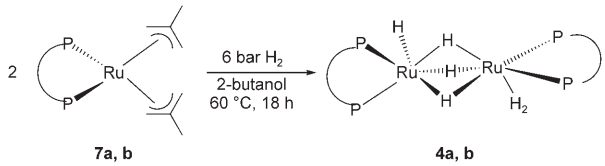

Scheme 1. Formation of complexes of type **4a** (100%) and **4b** (36%) by hydrogenation of allyl-type complexes **7a** (P_2 = dcpp) and **7b** (P_2 = dcpe).

The IR spectra of complexes **4a** and **4b** show characteristic bands that are readily assigned to terminal hydrides (Ru–H) and bridging hydrides (Ru-H-Ru), located for **4a** at $\tilde{\nu}$ 1990 and 1552 cm^{-1}, respectively. As other parts of the IR

spectrum of **4a** are dominated by the bands resulting from the dcpp ligands, the IR spectrum of the corresponding deuterated complex [D_6]-**4a** was also examined. The two bands for the terminal and bridging hydrides show an isotope shift of $\sqrt{2}$ in accordance with the Teller–Redlich rule.[25] In addition, a new band appears at 1719 cm^{-1} in the spectrum of [D_6]-**4a**, which can be assigned to the D–D stretching of a coordinated D_2 molecule. Even if ν_{H-H} cannot be determined exactly by the Teller–Redlich rule, which is valid for uncoupled oscillations only, this result indicates the presence of a σ-coordinated dihydrogen molecule in **4a**.

The ^{1}H NMR spectrum of **4a** shows a single averaged signal for all hydridic ligands as a slightly broad singlet centred at $\delta = -11.8$ ppm, which integrates for six H atoms at various relaxation delays. The chemical shift value has also been confirmed by ^{2}H NMR experiments with [D_6]-**4a**. When [D_6]-**4a** was generated in situ by charging a solution of **4a** in [D_8]toluene with D_2 gas in a Young NMR tube, the deuterium spectrum also revealed several signals between $\delta = 1.1$ and 1.9 ppm. These signals indicate H/D exchange by a C–H activation process at various positions of the dcpp ligands. The ^{31}P NMR signal of **4a**, which at room temperature is detected at $\delta = 69.5$ ppm, splits into two broad signals when the temperature is lowered to −80 °C. The high-field proton signal does not yet show significant decoalescence at this temperature. Owing to the fast exchange between classical and nonclassical hydrides even at low temperature, it was not possible to determine separate resonance frequencies for the individual hydridic ligands or to measure P–H coupling constants.

In order to further evaluate the nature of the hydridic ligands in complex **4a**, the minimum relaxation time T_1(min) was determined.[26] The values measured with a 400 MHz NMR spectrometer at various temperatures are graphically displayed in Figure 3. The T_1(min) for **4a** was determined as 53 ms at 271 K. A comparison with the values reported for other similar complexes confirms the presence of a nonclassical structure, which is usually associated with $T_1(\min) <$ 100 ms. An H–H distance of 104 pm (±1 pm based on instrumental errors) can be calculated from the T_1(min) measurement. Owing to dynamic exchange with the other hydride signals, this value can be regarded only as the upper limit for the distance in the coordinated H_2 moiety, however.

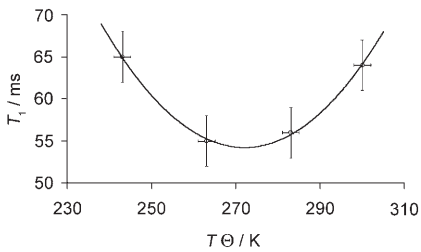

Figure 3. Temperature-dependent evolution of the T_1 values measured for **4a**. T_1/ms (Δ3 ms) [T/K (Δ2 K)]: 64 [300], 56 [283], 55 [263], 65 [243], 108 [223].

Additional evidence for the presence of a σ-coordinated hydrogen molecule is provided by the reaction of complex **4a** with molecular nitrogen to form the complex [H-(dcpp)Ru(μ-H)$_3$Ru(dcpp)(N_2)] (**8**).[1,3,4] After exposure of a [D_8]toluene solution of **4a** to a nitrogen stream in a Young valve NMR tube, the high-field region of the ^{1}H NMR spectrum shows, together with a small signal for the starting complex, one apparent doublet at $\delta = -9.2$ ppm ($\Delta\nu$ = 53 Hz), one broad signal at $\delta = -15.5$ ppm and one triplet at $\delta = -19.4$ ppm (t, ^2J(H,P) = 33 Hz). The ^{31}P NMR shows two signals of equal intensity at $\delta = 75.1$ ppm (s) and $\delta = 47.1$ ppm (s) and reveals 9 % of the starting material at $\delta = 68$ ppm (s). The reaction is reversible and compound **4a** is quantitatively restored when the same solution is exposed to hydrogen gas. Interestingly, **4a** can also easily be converted to **8** in the solid state under 14 bar nitrogen pressure, indicating that the coordination sphere in both solution and solid state is identical.

The solid-state structure of the ruthenium hydride **4a** was determined by single-crystal X-ray structure analysis. Crystals of **4a**, suitable for X-ray investigation, were obtained by slow evaporation of a hexane solution under hydrogen atmosphere. Figure 4 depicts a graphical representation of the molecular structure and Table 1 summarises selected bond lengths and angles.[27] Notably, all hydrogen atoms in the coordination sphere of the ruthenium centres could be located and fully refined.

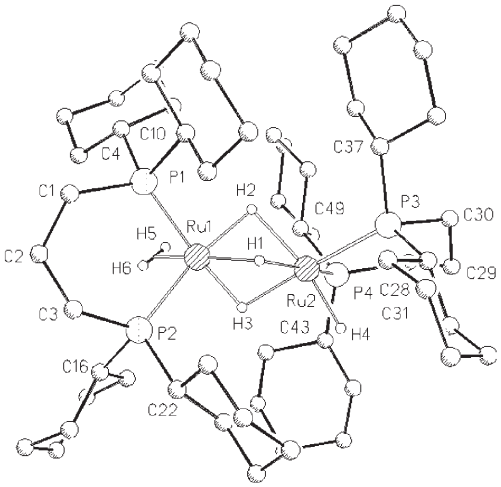

Figure 4. ORTEP diagram of the molecular structure of **4a** as determined by single X-ray diffraction.

The dimeric structure of **4a** is made of two slightly distorted octahedra, whose centres are occupied by the two ruthenium atoms. The phosphine groups exhibit an anticline arrangement, which minimises the steric effect of the cyclohexyl groups in the backbones. The bite angle measured for the two dcpp ligands in **4a** (≈95°) is slightly larger than previously reported for **7a** (≈91.3°).[24] The distances between the bridging hydrides and the ruthenium centres are significantly longer than those measured for the remaining hydro-

Table 1. Selected distances and angles of complex **4a**.

Distances [Å]		Angles [°]			
Ru1–H1	1.83 (4)	H1-Ru1-H2	71.4 (15)	H6-Ru1-H1	70 (2)
Ru1–H2	1.78 (3)	H2-Ru1-H3	82.8 (14)	H3-Ru1-H1	76.7 (16)
Ru1–H3	1.73 (3)	H5-Ru1-H3	157 (2)	H5-Ru1-H2	87.8 (18)
Ru1–H5	1.68 (4)	H5-Ru1-H3	91.3 (18)	H6-Ru1-H2	117 (2)
Ru1–H6	1.63 (6)	H6-Ru1-H3	98 (2)	P1-Ru1-P2	95.32 (3)
Ru2–H1	1.84 (4)	P1-Ru1-Ru2	129.8 (18)	P2-Ru1-Ru2	121.91 (2)
Ru2–H2	1.91 (3)				
Ru2–H3	1.81 (3)	H1-Ru2-H2	68.4 (15)	H2-Ru2-H3	77.2 (13)
Ru2–H4	1.61 (3)	H3-Ru2-H1	74.5 (16)	H4-Ru2-H1	102.3 (17)
H5–H6	0.833	H4-Ru2-H2	166.4 (14)	H4-Ru2-H3	90.9 (15)
Ru1–P1	2.272 (7)	P3-Ru2-P4	95.91 (3)	P3-Ru2-Ru1	134.73 (2)
Ru1–P2	2.274 (7)	P4-Ru2-Ru1	118.21 (2)		
Ru2–P3	2.266 (7)				
Ru2–P4	2.254 (7)	Ru1-H1-Ru2	88.8		
		Ru1-H2-Ru2	88.0		
Ru1–Ru2	2.569 (7)	Ru1-H3-Ru2	93.3		

gen atoms. Most significantly, two hydrogen atoms were located in an arrangement characteristic of a coordinated H_2 molecule at Ru1 with an H–H distance of 0.83 Å. Considering the dynamic behaviour of **4a** in solution, this value is in full agreement with the upper limit derived from T_1 measurements. The H_2 moiety is almost fully aligned with the plane described by the phosphorus atom P2, the ruthenium centre Ru1, and the bridging hydride H2. This arrangement may be explained in terms of a favourable overlap between the σ* on H_2 and a filled d orbital on the metal, which allows most efficient backbonding.

Comparison of the structure of complex **4a** with the known dimeric ruthenium hydride complexes **9** and **10**, containing nonchelating phosphine ligands (Figure 5)[28] contributes to a better understanding of how the electronic and structural environment around the metal centre affects the hydrogen coordination. It has been shown that complex **9**, with its PPh_3 ligand, must be formulated as a nonclassical dihydrogen complex,[28a] whereas complex **10**, with the P*i*Pr_3, ligand adopts the form of a classical dihydride.[28b] Following classical arguments, this difference arises because the stronger basicity of the P*i*Pr_3 ligand favours back donation into the antibonding orbital of the coordinated σ-H_2 ligand, which leads finally to rupture of the H–H bond. However, based on the basicity of the phosphine ligands, a classical dihydride structure would also be expected for complex **4a** (dcpp: $pK_a \approx 10$; P*i*Pr_3: $pK_a \approx 8$; PPh_3: $pK_a = 2.7$),[29] which is obviously not in agreement with the experimentally determined structure in the solid state and in solution.

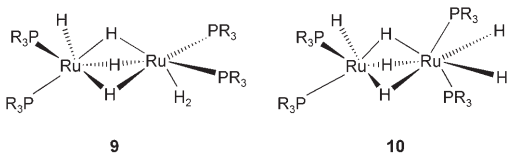

9 10

Figure 5. Dinuclear ruthenium hydride complexes **9a** (R = Cy), **9b** (R = Ph), and **10** (R = *i*Pr) containing nonchelating phosphine ligands.

A closer inspection of the molecular structures of the three complexes reveals that the coordination geometry in the P-Ru-P unit plays a more important role in defining the bonding situation of the Ru–H_2 moiety than does the ligands basicity.[10] It is well known that changes in P-M-P coordination geometry can influence the electronic properties at the metal centre more strongly than purely electronic factors through changes in the hybridisation[30a] or by changing the overlap of the lone pair of the donor with the M–P trajectory.[30b] In the present case, the -$(CH_2)_3$- backbone in dcpp fixes the two donor units in a *cis* arrangement with a bite angle of 95.3 (P1-Ru1-P2) and 95.9° (P3-Ru2-P4), very similar to the one observed in **9b** (≈95°). The bulky P*i*Pr_3 ligands in **10** maximise their distance freely, thus widening the P-Ru-P angles to 113.10 (P1-Ru1-P2) and 106.75° (P3-Ru2-P4). Thus, the nonclassical structure in the dimeric complexes can be associated with the smaller bite angle, whereas the dihydride structure is adopted for larger bite angles. If the angle opens up fully to adjust a *trans* arrangement of the two donor ligands, the dimeric structures break up to form the monomeric complexes of type **1–3** in the presence of excess hydrogen. Naturally, this is not possible if the *cis* arrangement is permanently fixed as in the complexes with bidentate ligands.

In an attempt to generate monomeric nonclassical ruthenium hydride complexes with a chelating ligand framework, we turned our attention toward pincer-type ligands that allow a *trans* arrangement of two electron-rich and bulky phosphorous donor groups. In a one pot procedure, [Ru(cod)(metallyl)$_2$] **11** was hydrogenated (7 bar) at 50 °C in the presence of phosphine **12**. A reddish-brown solid precipitated from MeOH solution and was isolated by filtration of the reaction mixture at room temperature.

^{1}H NMR and ^{31}P NMR analysis in [D_8]THF solution confirmed the presence of the new nonclassical polyhydride complex [Ru(dtbpmb)(H_2)$_2$H] **5** (dtbpmb = 1,3-bis((di-*tert*-butylphosphino)methyl)benzyl) as major reaction product, together with small amounts (<10%) of unidentified side products. In solution the nonclassical trihyride **13** is generated owing to loss of H_2 (38%). The two dihydrogen complexes **5** and **13** result from coordination of the ligand and intramolecular C–H activation at the 2-position in the aromatic ring (Scheme 2).[11] At room temperature the five hydrogen atoms in the coordination sphere of the ruthenium centre of complex **5** give rise to an average broad signal centred at $\delta = -9.21$ ppm, while the equivalent phosphorous atoms lead to a singlet at $\delta = +107.8$ ppm in the ^{31}P NMR spectrum. ^{1}H NMR experiments performed at low tempera-

ture (−80 °C) allowed identification of the individual signals for the Ru–H (δ = −11.83 ppm, t, ^2J(H,H) = 17.7 Hz) and Ru–H_2 (δ = −7.01 and −5.04 ppm, broad signals) moiety. The high-field ^{1}H NMR signals for [Ru(dtbpmb)(H_2)H] **13** also reveal Ru–H (δ = −35.2 ppm) and Ru–H_2 (δ = −3.67 ppm) units. The corresponding ^{31}P resonance is found at δ = 104.3 ppm. The ratio of the nonclassical pentahydride to trihydride complexes was determined to be **5**:**13** = 58:42. The treatment of the NMR sample in [D_8]THF with a stream of H_2 at room temperature for 10 minutes gives exclusively compound **5** from **13**. The reaction of **5** with

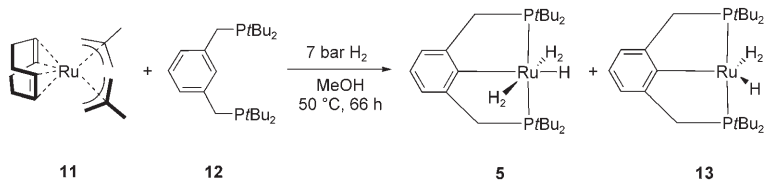

Scheme 2. Formation of **5** by hydrogenation of [Ru(cod)(metallyl)$_2$] (**11**) in presence of the PCP pincer precursor phosphine **12**. The pentahydride **5** is the main product formed under hydrogen atmosphere. Trihydride **13** is generated in solution by H_2 loss.

CD_2Cl_2 at room temperature gave the known ruthenium complex [Ru(dtbpmb)HCl] **16** according to ^{1}H and ^{31}P NMR (Scheme 3.[23a,31]

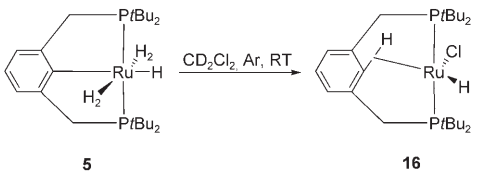

Scheme 3. Formation of [Ru(dtbpmb)HCl] **1**) at room temperature.

[Ru(cod)(metallyl)$_2$] **11** reacts cleanly under similar conditions with the direct hydrogenation route and the PNP pincer ligand dtbpmp **17** to give the complex [Ru(dtbpmp)H_2(H_2)] **6** (Scheme 4). Complex **6** is isolated directly from the reaction mixture by filtration at room temperature; it is a light-brown, microcrystalline powder obtained good yields under optimised conditions. In contrast to the situation in complex **5**, the neutral two-electron donor group of the pyridine moiety in **17** results in the coordination of two classical hydrides and one molecular hydrogen ligand. At room temperature, the ^{1}H NMR spectrum has a signal at δ = −7.3 ppm (t, 4H, ^2J(H,P) = 13.2 Hz) and upon cooling the sample to −80 °C the triplet changes to a broad signal. T_1(min) was found to be 77 ms at θ_{min} = 228 K (Figure 6), resulting in an upper limit of 111 pm (± 1 pm, based on instrumental error) for the H–H distance in the H_2 moiety.

The dihydrogen ligand in complex **6** can be replaced by N_2, but the reactivity of **6** differs significantly from that of complexes **1**–**4** (Scheme 5). Firstly, the ligand exchange is

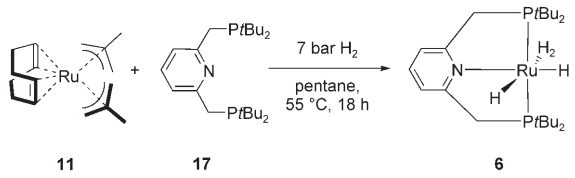

Scheme 4. Direct hydrogenation of [Ru(cod)(metallyl)$_2$] (**11**) in the presence of dtbpmp (**17**) to give the nonclassical ruthenium hydride complex **6**.

relatively slow (66 % conversion after 90 min) and small amounts of unreacted **6** can be detected by ^{1}H NMR spectroscopy even after bubbling a stream of nitrogen through a solution of **6** in [D_8]toluene overnight. Furthermore, the complex [Ru(dtbpmp)H_2(N_2)] **18** (we assume it to be monomeric but a dinitrogen-bridged dimer cannot be excluded of course; ^{31}P NMR: δ =

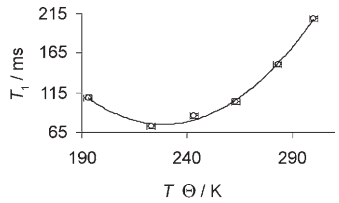

Figure 6. T_1 values as a function of temperature determined for [Ru(dtbpmp)H_2(H_2)] **6**. T_1/ms (Δ3 ms) [T/K (Δ2 K)]: 209 [300], 151 [283], 104 [263], 86 [243], 73 [223], 109 [193].

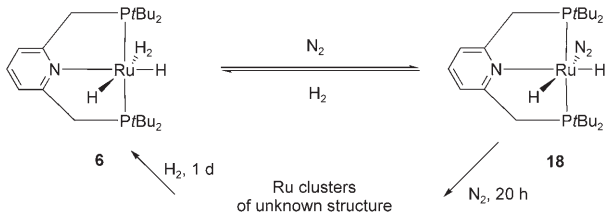

Scheme 5. Reversible formation of dinitrogen complex **18** and ruthenium clusters from **6** under N_2 and H_2 atmosphere.

+99.6 ppm; ^{1}H NMR: δ = −4.6 (t, ^2J(H,P) = 16.81 Hz) and −12.8 ppm) appears to be unstable and converts to a dynamic system of presumably polynuclear complexes as indicated by two sets of broad signals at δ = +81–74 and +70–65 ppm (see Supporting Information for details). This process is fully reversible and complex **6** is restored quantitatively (by NMR) under hydrogen atmosphere.

^{1}H NMR studies of the long term stability of complex **6** in aromatic solvents reveal an interesting H/D exchange pro-

cess in [D_8]toluene or C_6D_6, whereby complex **6** incorporates deuterium from the solvents into the PNP pincer backbone ([D_x]-**6**, Scheme 6). Preferably, the C4 position of the

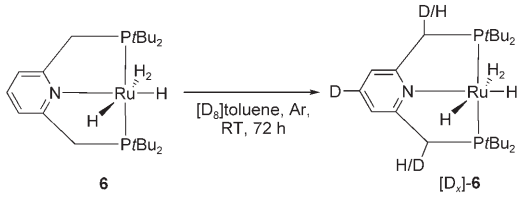

Scheme 6. Formation of [D_x]-Ru(dtbpmp)H_2(H_2) [D_x]-**6** starting from **6** with [D_8]toluene at room temperature within 72 h.

pyridyl system (δ = 6.5 ppm; >95% D) and the benzylic positions (δ = 3.1 ppm; ≈25% D) are deuterated within 72 h at room temperature. Interestingly, the hydride area of the ^{1}H NMR still shows hydridic signal at this stage. This indicates that a slow H/D exchange between **6** and the solvent is followed by a rapid exchange at the pincer backbone from the intermediate ruthenium deuteride. After three weeks, the sealed NMR sample also shows a decrease of signal intensity in the *tert*-butyl resonances and a significant increase of the solvent residue H signal is also detected. The ^{31}P NMR spectra of this sample still shows mainly the signal of **6** at δ = 109 ppm (>90%), with additional small signals between δ = 107 and 88 ppm. After 3.5 months the ^{31}P NMR spectrum of the same sample remains identical, but the ^{1}H NMR spectrum shows further decrease of the signal intensity in all molecular parts including the hydride moiety and an increase of the solvent residue signal. In a further experiment we performed the deuteration of **6** in C_6D_6 at 50 °C for 48 h. Analysis by ^{2}H NMR confirmed unequivocally the incorporation of deuterium in the hydride, aliphatic, and aromatic parts, and ^{1}H NMR spectroscopy revealed that >90% of the hydrogen atoms in **6** are substituted by deuterium in all positions.

Similar results were obtained when the complex synthesis was performed using D_2 gas instead of H_2. Again the C4 position (>95% D) and the benzylic positions (≈25% D) were deuterated as indicated by comparison of the IR spectra (Figure 7) and NMR of **6** and [D_x]-**6**. The IR spectra of the non-deuterated complex **6** show bands characteristic of ruthenium hydrides at 1990, 1892, and 1700 cm^{-1} (ν(Ru–H)) and at 2095 cm^{-1} (ν(Ru–H_2)). Moreover, the spectra of [D_x]-**6** includes further bands at 2247, 2199, and 2151 cm^{-1} which can be assigned as ν(CD_{ar}) bands by comparison with the ν(CH_{ar}) bands according to the Teller–Redlich rule.[25] The expected bands between 1488 and 1202 cm^{-1} for ruthenium deuterides could not be detected in the indicated area. These results show that a synthesis of [D_4]-**6** seems impossible because during the synthesis under D_2 gas rapid H/D scrambling occurs and finally a partly deuterated pincer backbone is obtained and the expected ruthenium deuterides are exchanged to ruthenium hydrides.

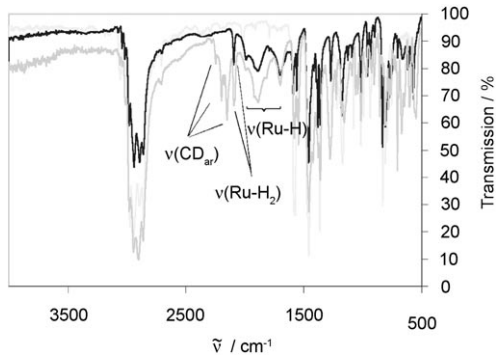

Figure 7. Comparison of the IR spectra of [Ru(dtbpmp)H_2(H_2)] (**6**) (black), [D_x]-Ru(dtbpmp)H_2(H_2) [D_x]-**6** (grey) and the free ligand dtbpmp **17** (light grey).

Conclusion

In summary, we have presented the synthesis and characterisation of two types of nonclassical ruthenium hydride complexes containing chelating ligands with defined coordination geometries. The straightforward preparation is achieved by hydrogenation of readily available bis-methallyl complexes. Dimeric complexes of type **4** are obtained with bidentate *cis* chelating phosphine ligands, whereas monomeric complexes **5** and **6** can be generated with tridentate PCP and PNP pincer ligands. The presence of coordinated dihydrogen molecules was confirmed by X-ray structure analysis and IR and NMR spectroscopic techniques. The stable coordination of the H_2 molecule in the binuclear polyhydride complexes is strongly influenced by the coordination geometry, which appears to play a more decisive role than the basicity of the P donor groups.

The monomeric complex **6** with a PNP pincer ligand shows an interesting reactivity in particular relating to C–H bond activation processes. Whereas it is typically the acidic benzylic position that is activated in other ruthenium complexes of this ligand class,[32] complex **6** shows a strong preference for the activation of aromatic C–H bonds. The implication of this reactivity for catalysis is currently under investigation in our laboratories and will be reported separately.

Experimental Section

General: All reactions were performed under Ar, H_2, D_2 or N_2 atmospheres using Schlenk or glove-box techniques. Solvents and substrates were purchased from Aldrich, Acros, and Strem and were purified according to standard procedures.[33] The PNP ligand dtbpmp **17** was synthesised according to the procedure by Milstein et al.[23e] and Hartwig and Kawatsura.[34] The allyl complexes **7a** and **7b** were prepared according to a previously reported synthesis.[24] The syntheses of the ruthenium hydrides were carried out in a modified thick-walled glass reactor (Büchi Glas Uster Miniclave), comparable with a Fischer–Porter bottle.

SAFETY WARNING: The use of pressurised gases can be hazardous and must only be carried out with suitable equipment and under appropriate safety precautions.

[H(dcpp)Ru(μ-H)$_3$Ru(dcpp)(H_2)] (4a): Allyl complex **7a** (259 mg, 0.4 mmol) and hexane (5 mL) were introduced in a thick-walled glass reactor, which was subsequently charged with H_2 (7 bar). The light grey

suspension was heated under stirring to 55 °C for 18 h. After cooling to room temperature, the autoclave was vented and the solution was filtered by cannula. Complex **4a** was obtained as a dark orange powder (216 mg, 0.2 mol; >99 %) after drying under H_2 atmosphere. Suitable crystals for X-ray structure analysis were obtained by slow recrystallisation from the mother liquor. For these data, please see Supporting Information. M.p. 230 °C (decomp); ^{1}H NMR (300 MHz, C_6D_6, 25 °C): δ = 2.4–1.1 (m, 106 H; dcpp), −11.8 ppm (br, 6 H, Ru-H_n); ^{13}C NMR (75 MHz, [D_8]toluene, 25 °C): δ = 39.8 (t, 8 C; P*C*H of Cy), 29.3 (d, 16 C;, *o*-CH_2 of Cy), 28.0 (t, 16 C; *m*-CH_2 of Cy), 27.4 (s, 8 C;, *p*-CH_2 of Cy), 24.5 (s, 2 C; $PCH_2CH_2CH_2P$), 24.2 ppm (t, 4 C;, $PCH_2CH_2CH_2P$); ^{31}P NMR (122 MHz, C_6D_6, 25 °C): δ = 69.5 ppm (s); IR (KBr): $\tilde{\nu}$ = 2927 (s; ν_{CH_2}), 2846 (s; ν_{CH_2}), 1990 (w; Ru-H), 1552 (w; Ru-H-Ru), 1445 (s; δ_{CH_2}), 1415 cm^{-1} (m; δ_{CH_2}); elemental analysis calcd (%) for $C_{54}H_{106}P_4Ru_2$ (1081.5): C 59.97, H 9.88, P 11.46, Ru 18.69; found: C 59.67, H 9.74, P 11.50, Ru 18.83.

[D(dcpp)Ru(μ-D)$_3$Ru(dcpp)(D$_2$)] ([D$_6$]-4a): Prepared as **4a** by the use of deuterium gas. ^{2}H NMR (400 MHz, hexane, 25 °C): δ = 1.48–0.68 (dcpp), −12.22 ppm (s, 6 D; Ru-D); IR (KBr): $\tilde{\nu}$ = 2924 (s; ν_{CH_2}), 2846 (s, ν_{CH_2}), 2652 w, 1445 (s; δ_{CH_2}), 1415 m (s; δ_{CH_2}).

Reaction of [H(dcpp)Ru(μ-H)$_3$Ru(dcpp)(H$_2$)] (4a) with deuterium gas to [D$_6$]-4a: A Young NMR tube containing a [D_8]toluene solution of **4a** was cooled with liquid nitrogen. After evacuation the tube was slowly charged with D_2 (0.5 bar) and warmed up to room temperature. The ^{1}H NMR spectrum was measured over 10 minutes. ^{1}H NMR (300 MHz, [D_8]toluene, 25 °C): δ = 1.11–2.36 ppm (dcpp), (no hydride signal observed in the hydride region); ^{31}P NMR (122 MHz, [D_8]toluene, 25 °C): δ = 68.1 ppm (s).

Reaction of [H(dcpp)Ru(μ-H)$_3$Ru(dcpp)(H$_2$)] (4a) with nitrogen gas to 8: A Young NMR tube containing [D_8]toluene solution of **4a** was slowly charged with N_2 (0.5 bar) at room temperature. ^{1}H NMR (300 MHz, [D_8]toluene, 25 °C): δ = 1.17–3.21 (br; dcpp), −9.20 (d, ^2J(H,P) = 53 Hz; μ-*H*), −15.50 (br; μ-*H*), −19.41 ppm (t, ^2J(H,P) = 33 Hz; Ru-$H_{term.}$); ^{31}P NMR (122 MHz, [D_8]toluene, 25 °C): δ = 47.3 (s), 75.0 ppm (s), the spectrum also revealed 9 % starting material at δ = 68.0 ppm (s).

[H(dcpe)Ru(μ-H)$_3$Ru(dcpe)(H$_2$)] (4b): Starting from the allyl precursor **7b** the same procedure used for **4a** was followed. Conversion: 36 %. ^{1}H NMR (300 MHz, C_6D_6, 25 °C): δ = 0.8–2.3 (dcpe), −11.3 ppm (br, 6 H; Ru-H_n); ^{31}P NMR (122 MHz, C_6D_6, 25 °C): δ = 114.3 ppm; (s); IR (KBr): $\tilde{\nu}$ = 2043 (w; Ru-H), 1653 cm^{-1} (w; Ru-H-Ru).

[Ru(dtbpmb)(H$_2$)$_2$H] (5): A mixture of [Ru(cod)(metallyl)$_2$] (**11**) (0.118 g, 0.369 mmol) and 1,3-bis(di-*tert*-butylphosphinomethyl)benzene (**12**) (0.146 g, 0.370 mmol) in methanol (5 mL) was introduced in a thick-walled glass autoclave, which was subsequently charged with H_2 (7 bar) and stirred for 66 h at 50 °C. After cooling to room temperature, the autoclave was vented and the solution was filtered by cannula and washed twice with small amounts of methanol. Complex **5** was obtained as a reddish brown powder (80 mg, 43 %) after drying under H_2 atmosphere at 50 °C. M.p. 179.2–180.5 °C; ^{1}H NMR (300 MHz, [D_8]THF, 25 °C): δ = 6.85 (d, ^3J(H,H) = 7.46 Hz, 2 H; Ar-H), 6.57 (t, ^3J(H,H) = 7.46 Hz, 1 H; Ar-H), 3.33 (virtual t, ^2J(H,P) = 4 Hz, 4 H; CH_2), 1.22 (virtual t, ^3J(H,P) = 6.10 Hz, 36 H; CH_3), −9.21 ppm (br, 5 H; Ru-H); ^{31}P NMR (122 MHz, [D_8]THF, 25 °C): δ = 107.79 ppm; ^{1}H NMR (300 MHz, [D_8]THF, −80 °C): δ = 6.76 (d, ^3J(H,H) = 7.33 Hz, 2 H; Ar-H), 6.50 (t, ^3J(H,H) = 7.33 Hz, 1 H; Ar-H), 3.22 (br, 4 H; CH_2), 1.12 (br, 36 H; CH_3), −5.05 (br, 2 H; Ru-H_2), −7.012 (br, 2 H; Ru-H_2), −11.8 ppm (t, ^2J(H,H) = 17.7 Hz, 1 H; Ru-H); ^{31}P NMR (122 MHz, [D_8]THF, −80 °C): δ = 109.05 ppm (s); IR (KBr): $\tilde{\nu}$ = 2156 (w; Ru-H), 2084 (w; Ru-H), 2013 cm^{-1} (w; Ru-H); elemental analysis calcd (%) for $C_{24}H_{48}P_2Ru$ (499.7): C 57.69, H 9.68, P 12.40, Ru 20.23; found: C 56.45, H 9.44, P 12.19 (sum 78.08 % found); found atom ratio number by CHN: $C_{24}H_{47.8}P_{2.0}$ $Ru_{1.1}$; detection of [Ru(dtbpmb)(H$_2$)H] **13** in solution: ^{1}H NMR (300 MHz, [D_8]THF, −80 °C): δ = 6.94 (d, ^3J(H,H) = 7.33 Hz, 2 H; Ar-H), 6.62 (t, ^3J(H,H) = 7.33 Hz, 1 H; Ar-H), 3.42 (br, 4 H; CH_2), 1.12 (br, 36 H; CH_3), −3.67 (br, 2 H; Ru-H_2), −35.19 ppm (br, 1 H; Ru-H); ^{31}P NMR (122 MHz, [D_8]THF, −80 °C): δ = 104.30 ppm (s).

[Ru(dtbpmp)H$_2$(H$_2$)] (6): A Büchi glass autoclave, equipped with a stirring bar, was filled with [Ru(cod)(metallyl)$_2$] (**11**) (281 mg, 0.88 mmol; 1 equiv), dtbpmp (**17**) (364 mg, 0.92 mmol; 1.05 equiv) and degassed *n*-pentane (12 mL). The autoclave was flushed with 2 bar H_2 gas (or D_2 gas) at room temperature, then the temperature was increased to 55 °C (oil bath), and the H_2 pressure was stabilised at 7 bar. The reaction was stirred for 18 h, cooled to room temperature and the H_2 pressure was decreased to 1 bar. The red solution was filtered through a cannula under an H_2 stream and the remaining solid was washed under an H_2 stream with *n*-pentane to give a yellow-brown solid, which was primarily stored under 1 bar hydrogen in the autoclave. The product was transferred into a dry Schlenk tube using a glove box and further dried under an H_2 stream. Finally it was stored under 1 bar hydrogen in an additionally sealed (parafilm) Schlenk tube at −20 °C (323 mg, 74 %). ^{1}H NMR (300 MHz, C_6D_6, 25 °C): δ = 6.8 (t, 1 H, ^3J(H,H) = 7.7 Hz; pyridine-H4), 6.6 (d, 2 H, ^3J(H,H) = 7.9 Hz; pyridine-H3,5), 3.1 (virtual t, 4 H, ^2J(H,P) = 3.2 Hz; CH_2P), 1.3 (virtual t, 36 H, ^3J(H,P) = 6.1 Hz; PC(CH_3)$_3$), −7.3 ppm (t, 4 H, ^2J(H,H) = 13,2 Hz; Ru-*H*, Ru-H_2); ^{13}C NMR (75 MHz, C_6D_6, 25 °C): δ = 164 (d virtual t, ^2J(C,P) = 4.8 Hz; pyridine-C2,6), 133 (s, pyridine-C4), 118 (m, pyridine-C3,5), 41 (d virtual t, ^1J(C,P) = 4.9 Hz; CH_2P), 34 (d virtual t, ^1J(C,P) = 6.7 Hz; PC(CH_3)$_3$), 30 ppm (vt, ^2J(C,P) = 3.4 Hz; PC(CH_3)$_3$); ^{31}P NMR (122 MHz, C_6D_6, 25 °C): δ = 109.5 ppm (s); IR (KBr) $\tilde{\nu}$ = 3074 (w, ν; CH_{ar}), 3041 (w, ν; CH_{ar}), 3018 (w, ν; CH_{ar}), 2983 (w, ν; CH_2), 2940 (s, ν; CH_2), 2893 (s, ν; CH_2), 2862 (s, ν; CH_2), 2095 (w, ν; Ru-H_2), 1990–1700 (m, ν; Ru-H), 1592 (m, ν; C=N), 1562 (m, ν; C=C), 1459 (s, δ; CH_2), 1382 (s, δ; *t*Bu), 1363 (s, δ; *t*Bu), 1180 (m, ν; C-P), 833 cm^{-1} (s, δ; CH_{ar}); detection of T_1(min) of the hydride signal: (400 MHz, [D_8]toluene, 25 °C): δ = −7.3 ppm (t, 4 H, ^2J(H,P) = 13.2 Hz); T_1(min) = 77 ms (θ_{min} = 228 K), *r*(H-H) = 111 pm; elemental analysis calcd (%) for $C_{23}H_{47}NP_2Ru$ (500.7): C 55.18, H 9.46, N 2.80, P 12.37, Ru 20.19; found: C 54.11, H 9.22, N 2.64, P 11.81, Ru 19.82 (sum: 97.6 % found); found atom ratio number by CHN: $C_{23}H_{46.7}N_{1.0}P_{2.0}Ru_{1.0}$.

[D$_x$]-[Ru(dtbpmp)H$_2$(H$_2$)] [D$_x$]-6: Prepared as **6** by the use of deuterium gas to give a yellow-brown solid (118 mg, 54 %). ^{1}H NMR (300 MHz, C_6D_6, 25 °C): δ = 6.8 (t, 0.1 H, ^3J(H,H) = 7.7 Hz; pyridine-H4), 6.6 (d, 2 H, ^3J(H,H) = 7.9 Hz; pyridine-H3,5), 3.1 (vt, 3 H, ^2J(P,H) = 3.2 Hz; CH_2P), 1.3 (vt, 36 H, ^3J(P,H) = 6.1 Hz; PC(CH_3)$_3$), −7.3 ppm (t, 4 H, ^3J(H,H) = 13.2 Hz; Ru-*H*, Ru-H_2); ^{2}H NMR (600 MHz, C_6D_6, 25 °C): δ = 6.8 (s, weak; pyridine-D4), 6.6 (s, weak; pyridine-D3,5), 3.1 (s; CD_2P), 1.3 (s; PC(CD_3)$_3$), −7.3 ppm (s; Ru-*D*, Ru-D_2); ^{13}C NMR (75 MHz, C_6D_6, 25 °C): δ = 133 (s; pyridine-C4), 164 (pyridine-C2,6), 118 (m; pyridine-C3,5), 41 (PC(CH_3)$_3$), 33 (CH_2P), 30 ppm (PC(CH_3)$_3$); ^{31}P NMR (122 MHz, C_6D_6, 25 °C): δ = 109.1 ppm (s); IR (KBr): $\tilde{\nu}$ = 3012 (w, ν; CH_{ar}), 2983 (s, ν; CH_2), 2946 (s, ν; CH_2), 2900 (s, ν; CH_2), 2863 (s, ν; CH_2), 2247 (w, ν; CD_{ar}), 2199 (w, ν; CD_{ar}), 2151 (w, ν; CD_{ar}), 2094 (w, ν; Ru-H_2), 2000–1700 (m, ν; Ru-H), 1582 (m, ν; C=N), 1546 (m, ν; C=C), 1458 (s, δ; CH_2), 1362 (s, δ; *t*Bu), 707 cm^{-1} (s, δ; CH_{ar}).

Reaction of [Ru(dtbpmp)H$_2$(H$_2$)] (6) with C$_6$D$_6$ to form highly deuterated [D$_x$]-6: A Young Teflon capped NMR tube was filled with **6** (20 mg, 39.9 μmol) and C_6D_6 (0.5 mL) was added. The red solution was stirred at 50 °C for 2 d, cooled to RT, and the ^{1}H NMR and ^{31}P NMR spectra were measured manually locked on C_6D_6. Deuteration degree: >90 %; ^{1}H NMR (300 MHz, C_6D_6, 25 °C): δ = 6.8 (residue; pyridine-H4), 6.6 (residue; pyridine-H3,5), 3.1 (residue; CH_2P), 1.3 (residue; PC(CH_3)$_3$), −7.3 ppm (residue; Ru-*H*, Ru-H_2); ^{2}H NMR (600 MHz, C_6D_6, 25 °C): δ = 6.8 (s; pyridine-D4), 6.6 (s; pyridine-D3,5), 3.1 (s; CD_2P), 1.3 (s; PC(CD_3)$_3$), −7.3 ppm (s; Ru-*D*, Ru-D_2); ^{31}P NMR (122 MHz, C_6D_6, 25 °C): δ = 108.1 ppm (s).

Reaction of [Ru(dtbpmp)H$_2$(H$_2$)] (6) with nitrogen gas to form [Ru(dtbpmp)H$_2$(N$_2$)] (18): A Young Teflon-capped NMR tube containing a dark red solution of **6** (20 mg, 39.9 μmol) in [D_8]toluene (0.6 mL) was slowly bubbled with N_2 at room temperature. ^{1}H and ^{31}P NMR spectra were measured after 90 min (red solution) and 20 h (black mixture). The black mixture was then bubbled with H_2 for 1 d and ^{1}H and ^{31}P NMR spectra were recorded again. Conversion: 66 % (^{31}P NMR after 90 min); ^{1}H NMR (300 MHz, [D_8]toluene, 25 °C): δ = −4.6 (t, ^2J(H,P) = 16.81 Hz), −12.8 ppm (weak, broad); ^{31}P NMR (122 MHz, [D_8]toluene,

25 °C): $\delta = 99.6$ ppm (br s). For further tabulated values see Supporting Information.

Acknowledgements

Thanks are due to technical assistance of Reinhard Ettl, Conny Wirtz, and Bernd Waßmuth in the analytical departments of the MPI with NMR and IR experiments. Financial support of the Max-Planck-Society, the Fonds der Chemischen Industrie and the programme for Deutsch-Israelische Partnerschaft (DIP) is gratefully acknowledged.

[1] G. J. Kubas, R. R. Ryan, B. I. Swanson, P. J. Vergamini, H. J. Wasserman, *J. Am. Chem. Soc.* **1984**, *106*, 451–452.
[2] P. J. Jessop, R. H. Morris, *Coord. Chem. Rev.* **1992**, *121*, 155–284.
[3] a) G. J. Kubas, *Acc. Chem. Res.* **1988**, *21*, 120–128; b) G. J. Kubas, *Metal Dihydrogen and σ-Bond Complexes*, Kluwer Academic/Plenum Press, New York, **2001**.
[4] G. J. Kubas, *J. Organomet. Chem.* **2001**, *635*, 37–68.
[5] a) A. M. Kjoshi, K. S. MacFarlane, B. R. James, *J. Organomet. Chem.* **1995**, *488*, 161–167; b) G. Jia, W. S. Ng, C. P. Lau, *Organometallics* **1998**, *17*, 4538–4540.
[6] A. Dedieu, *Transition Metal Hydrides*, **1990**, VCH, Weinheim.
[7] M. Y. Darensburg, E. J. Lyon, J. J. Smee, *Coord. Chem. Rev.* **2000**, *206–207*, 533–561.
[8] D. M. Heinekey, W. J. Oldham Jr., *Chem. Rev.* **1993**, *93*, 913–926.
[9] G. J. Kubas, C. J. Burns, J. Eckert, S. Johnson, A. C. Larson, P. J. Vergamini, C. J. Unkefer, G. R. K. Khalsa, S. A. Jackson, O. Eisenstein, *J. Am. Chem. Soc.* **1993**, *115*, 569–581.
[10] K. Almeida Leñero, M. Kranenburg, Y. Guari, P. C. J. Kamer, P. W. N. M. van Leeuwen, S. Sabo-Etienne, B. Chaudret, *Inorg. Chem.* **2003**, *42*, 2859–2866.
[11] Preliminary results of this study have been communicated in part in S. Busch, W. Leitner, *Chem. Commun.* **1999**, 2305–2306.
[12] a) B. Chaudret, R. Poilblanc, *Organometallics* **1985**, *4*, 1722–1726; b) T. Arliguie, B. Chaudret, R. H. Morris, A. Sella, *Inorg. Chem.* **1988**, *27*, 598–599; c) A. F. Borowski, B. Donnadieu, J.-C. Daran, S. Sabo-Etienne, B. Chaudret, *Chem. Commun.* **2000**, 543–544; d) M. Grellier, L. Vendier, B. Chaudret, A. Albinati, S. Rizzato, S. Mason, S. Sabo-Etienne, *J. Am. Chem. Soc.* **2005**, *127*, 17592–17593.
[13] A. F. Borowski, S. Sabo-Etienne, M. L. Christ, B. Donnadieu, B. Chaudret, *Organometallics* **1996**, *15*, 1427–1434.
[14] a) B. Chaudret, G. Chung, O. Eisenstein, S. A. Jackson, F. J. Lahoz, J. A. Lopez, *J. Am. Chem. Soc.* **1991**, *113*, 2314–2316; b) G. Chung, T. Arliguie, B. Chaudret, *New J. Chem.* **1992**, *16*, 369–374; c) M. L. Christ, S. Sabo-Etienne, B. Chaudret, *Organometallics* **1994**, *13*, 3800–3804.
[15] Y. Guari, S. Sabo-Etienne, B. Chaudret, *J. Am. Chem. Soc.* **1998**, *120*, 4228–4229.
[16] R. P. Beatty, R. A. Paciello (Du Pont), WO 96/23802, priority date 08.08.1996.
[17] F. Delpech, S. Sabo-Etienne, B. Donnadieu, B. Chaudret, *Organometallics* **1998**, *17*, 4926–4928.
[18] For studies of stability of Chaudret's complex under catalytic conditions see: a) S. Busch, W. Leitner, *Adv. Synth. Catal.* **2001**, *343*, 192–195; b) Y. Guari, A. Castellanos, S. Sabo-Etienne, B. Chaudret, *J. Mol. Catal. A Chem.* **2004**, *212*, 77–82.
[19] T. R. Balderrain, R. H. Grubbs, *Organometallics* **1997**, *16*, 4001–4003.
[20] D. Giunta, M. Hölscher, C. W. Lehmann, R. Mynott, C. Wirtz, W. Leitner, *Adv. Synth. Catal.* **2003**, *345*, 1139–1145.
[21] P. Buskens, D. Giunta, W. Leitner, *Inorg. Chim. Acta* **2004**, *357*, 1969–1974.
[22] a) M. E. van der Boom, D. Milstein, *Chem. Rev.* **2003**, *103*, 1759–1792; b) M. E. van der Boom, L. Hassner, Y. Ben-David, D. Milstein, *Organometallics* **1999**, *18*, 3873–3884; c) M. E. van der Boom, M. A. Iron, O. Atasoylu, L. J. W. Shimon, H. Rozenberg, Y. Ben-David, L. Konstantinovski, J. M. L. Martin, D. Milstein, *Inorg. Chim. Acta* **2004**, *357*, 1854–1864.
[23] a) D. G. Gusev, M. Madott, F. M. Dolgushin, K. A. Lyssenko, M. Y. Antipin, *Organometallics* **2000**, *19*, 1734–1739; b) D. G. Gusev, F. M. Dolgushin, M. Y. Antipin, *Organometallics* **2000**, *19*, 3429–3434; c) D. G. Gusev, T. Maxwell, F. M. Dolgushin, K. A. Lyssenko, A. J. Lough, *Organometallics* **2002**, *21*, 1095–1100; d) E. J. Farrington, E. M. Viviente, B. S. Williams, G. van Koten, J. M. Brown, *Chem. Commun.* **2002**, 308–309; e) D. Hermann, M. Gandelman, H. Rozenberg, L. J. W. Shimon, D. Milstein, *Organometallics* **2002**, *21*, 812–818; f) Q. Major, A. J. Lough, D. G. Gusev, *Organometallics* **2005**, *24*, 2492–2501.
[24] C. Six, B. Gabor, H. Gorls, R. Mynott, P. Philipps, W. Leitner, *Organometallics* **1999**, *18*, 3316–3326.
[25] L. A. Woodward, *Introduction to the Theory of Molecular Vibrations and Vibrational Spectroscopy*, **1972**, Oxford University Press, London, p. 207–214.
[26] a) R. H. Crabtree, *Acc. Chem. Res.* **1990**, *23*, 95–101; b) W. Yao, J. W. Faller, R. H. Crabtree, *Inorg. Chim. Acta* **1997**, *259*, 71–76.
[27] For details see Supporting Information. CCDC-612003 contains the supplementary crystallographic data for this structure. These data can be obtained free of charge from the Cambridge Crystallographic Data Centre via www.ccdc.cam.ac.uk/data_request/cif.
[28] a) B. Chaudret, J. Devillers, R. Poilblanc, *Organometallics* **1985**, *4*, 1727–1732; b) K. Abdur-Rashid, D. G. Gusev, A. J. Lough, R. H. Morris, *Organometallics* **2000**, *19*, 1652–1660.
[29] D. Amoros, A. Jabri, G. P. A. Yap, D. G. Gusev, E. N. dos Santos, D. E. Fogg, *Organometallics* **2004**, *23*, 4047–4054 and references therein.
[30] a) P. Hofmann, C. Meier, U. Englert, M. U. Schmidt, *Chem. Ber.* **1992**, *125*, 353; b) W. Leitner, M. Bühl, R. Fornika, C. Six, W. Baumann, E. Dinjus, M. Kessler, C. Krüger, A. Rufinska, *Organometallics* **1999**, *18*, 1196–1206.
[31] C. J. Moulton, B. L. Shaw, *J. Chem. Soc. Dalton Trans.* **1976**, 1020–1024.
[32] a) J. Zhang, G. Leitus, Y. Ben-David, D. Milstein, *J. Am. Chem. Soc.* **2005**, *127*, 10840–10841; b) J. Zhang, G. Leitus, Y. Ben-David, D. Milstein, *Angew. Chem.* **2006**, *118*, 1131–1133; *Angew. Chem. Int. Ed.* **2006**, *45*, 1113–1115.
[33] D. D. Perrin, W. L. F. Armarego, *Purification of Laboratory Chemicals*, Pergamon Press, London.
[34] M. Kawatsura, J. F. Hartwig, *Organometallics* **2001**, *20*, 1960–1964.

Received: June 23, 2006
Published online: November 20, 2006

